SECOND EUROPEAN CONFERENCE ON EARTHQUAKE ENGINEERING
AND SEISMOLOGY, ISTANBUL AUG. 25-29, 2014

SEISMIC RESPONSE MITIGATION OF ELEVATED TANKS BY HDRB AND FPS ISOLATION SYSTEMS

Fabrizio PAOLACCI[1], Renato GIANNINI[2], Eren UCKAN[3], Bulent AKBAS[4], Daniele CORRITORE[5]

ABSTRACT

The aim of the paper is to evaluate the effectiveness of two isolation systems for the seismic protection of elevated steel storage tanks: High Damping Rubber Bearings (HDRB) and Friction Pendulum (FPS) isolators. As a case study, an elevated tank which collapsed during the Kocaeli Earthquake in 1999 at Habas Pharmaceutics plant in Turkey has been studied. A time-history analysis is conducted using lumped mass model to demonstrate the high base shear demand and inevitable collapse of support columns due to the insufficient shear strength. A proper design of HDRB and FPS isolator and a complete non-linear analysis of the isolated tanks prove the high effectiveness of both isolation systems for reducing the response of the tank. Results revealed that the tank with the FPS provides better performance compared to HDRB in terms of the isolation displacement convective base shear demands.

INTRODUCTION

The seismic response of elevated tanks has been widely investigated in the past. Typical structural configurations are realized by steel storage tanks upon steel or reinforced concrete columns. For slender support columns this kind of tanks has a natural capacity to filter the seismic action. In this case the isolation system does not represent a proper solution for the mitigation of the structural response; indeed, dissipative bracings could represent a more effective technique as demonstrated in literature by several authors [1]. On the contrary, in case of short columns, the positive filtering effect of the support could be limited. Moreover, in case of reinforced concrete (RC) supports, the high shear stiffness may induce premature shear failure in the columns, as shown in recent seismic event. For example, during Izmit earthquake (1999) in Turkey, a group of elevated tanks for the storage of liquefied oxygen were subjected to serious damages or collapsed [2].

This is a clear case in which base isolation technique could represent an effective solution to reduce the seismic response. The problem has been widely investigated even if only few applications have been realized. Based on the above depicted framework, this paper addresses the problem of elevated tanks with particular attention paid on steel storage tanks placed on short RC columns. The dynamic problem of elevated tanks subjected to seismic action is briefly described and formalized here.

The base isolation of a LNG steel tank supported by RC columns is presented and discussed. The analysed tank collapsed during 1999 Izmit earthquake for premature shear failure of columns. Firstly, the

[1] Ass. Prof. University Roma Tre, Rome, Italy, fabrizio.paolacci@uniroma3.it
[2] Full Prof. University Roma Tre, Rome, Italy, renato.giannini@uniroma3.it
[3] Assoc.Prof., Bosphorus University, Istanbul, eren.uckan@boun.edu.tr
[4] Assoc.Prof., Gebze Institute of Technology, Kocaeli, akbasb@gyte.edu.tr
[5] Ph.D Student University Roma Tre, Rome, Italy, daniele.corritore@uniroma3.it

response of fixed base configuration is analysed and discussed, which it will show the already known insufficient safety level against shear failure of the columns. Subsequently, in order to reduce seismic action on the tank two isolation systems are designed: HDRB and FPS. Their effectiveness will be analysed and compared.

1. DYNAMICS OF ELEVATED BASE ISOLATED CYLINDRICAL TANKS

The dynamics of cylindrical tanks subjected to a base motion has been extensively studied in the past by several authors. Starting from the earliest work of Housner [3], the hydrodynamic pressure induced by the liquid on the tank wall due to the base motion has been determined, taking into account the deformability of the tank wall; see for example [4, 5, 6].

In brief, the liquid mass can be imagined subdivided in two parts: an impulsive component, which follows the base motion and the deformability of the tank wall, and a convective component, whose oscillations cause superficial wave of different frequency with a very low percentage of mass (≅4%) relative to the higher modes; moreover, while in the slender tanks the most part of the liquid moves rigidly with the tank, in the broad tanks most of mass oscillates in the convective modes.

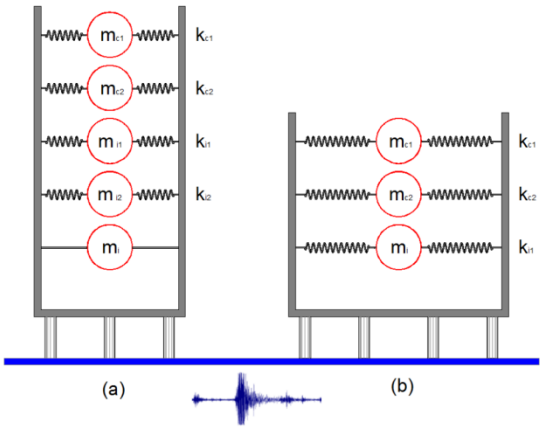

Figure 1. Equivalent spring-mass model of elevated tanks: (a) general, (b) broad tanks

Under the hypothesis of rigid tank, the impulsive and convective part of hydrodynamic pressure can be easily evaluated taking into account the effects of the ground acceleration and the relative acceleration of the tanks with respect to ground [7]. When the tank is placed upon RC columns or other type of supports, the dynamics is also influenced by the rotation at the tank base that has to be properly included in the equation of motions. Nevertheless, this effect can be neglected when the lateral displacements of the tank base are small.

On the contrary, the part, which depends on the deformability of the tank wall, can be determined solving a fluid-structure interaction problem, whose solution depends on the geometrical and mechanical characteristics of the tank: radius R, liquid level H, thickness s, liquid density ρ and elastic modulus of steel E. The problem can be uncoupled in infinite vibration modes, but only few of them have a significant mass. Thus, the impulsive mass is distributed among the first vibration modes of the wall [7].

On the basis of the above observations it can be drawn that the study of the hydrodynamic pressure in tanks subjected to a seismic base motion can be easily performed using the simple models shown in Fig.1, in which the liquid mass is lumped and subdivided in three components: rigid, impulsive and convective masses named m_i , m_{ik} (mass of k-th mode of the wall vibrations), m_{ck} (mass of k-th convective mode). The impulsive and convective masses are connected to the tank wall by springs of stiffness k_{ik} and k_{ck}. The total pressure is given by adding the effects of the mass m_i subjected to the base motion acceleration, of the masses m_{ik} subjected to the acceleration of the wall relative to the bottom of the thank, and of the masses m_{ck} subjected to the absolute acceleration.

In case of broad tanks the model shown in Fig.1(a) can be updated by the simplest model shown in Fig.1(b). In fact, the contribution of the higher order vibration modes is negligible and the entire impulsive mass is practically equal to the mass of the first vibration mode; moreover, because the distributions of the impulsive pressure, with and without wall deformability, are almost coincident, the effects of the impulsive action are simply taken into account by the response in terms of absolute acceleration of a simple oscillator

of mass m_i and stiffness k_i. Neglecting the higher convective modes effect, the model becomes a simple three degrees of freedom model shown in Fig.2 (a). The frequencies of the convective and impulsive modes are generally very different (tenths of a second against tens of seconds). This justifies the usual choice of neglecting the interaction between these two phenomena.

The idea of seismic protection of tanks through base isolation technique is not new. Starting from 1990's many works on this subject have been done [8, 9]. Unfortunately, few practical applications has been realized [10] and a limited number of experimental activity has been performed [7, 11].

Based on the above observations, a possible dynamic model of elevated tanks upon base isolation is shown in Fig. 2 (b).

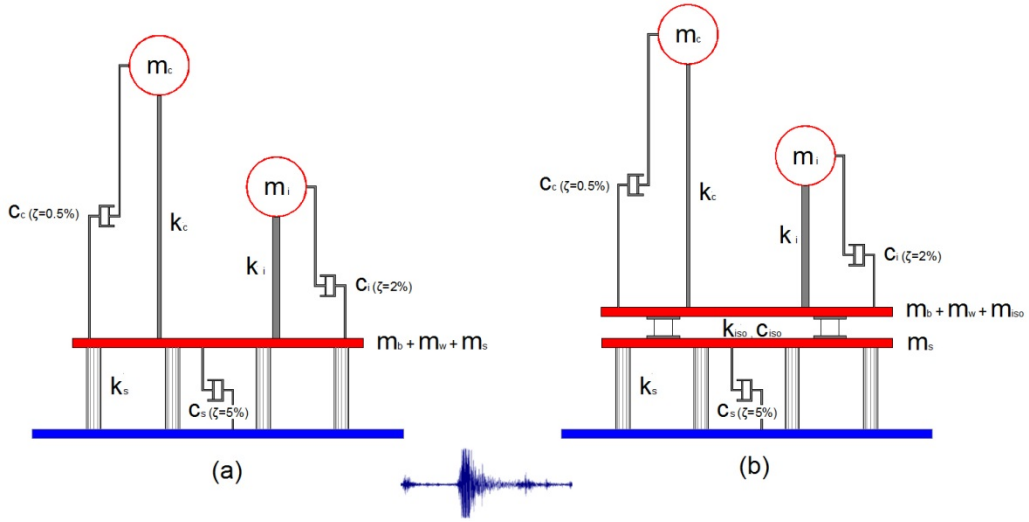

Figure 2. Lumped mass: (a) 3-DOF model of non –isolated elevated tanks, (b) 4-DOF model of isolated elevated tanks

The vibration period of the impulsive component of pressure generally falls in the maximum amplification field of the response spectrum, whereas the convective period T_c is usually very high and thus associated with a low amplification factor. This implies a high effectiveness of the base isolation system, which can reduce highly the base shear due to the impulsive pressure component. Neglecting the influence of the lateral deformation of wall and support, the period of the isolated structure is approximately given by:

$$T_{iso} \approx 2\pi \sqrt{\frac{m_i + m_s + m_b + m_w}{k_{iso}}} \qquad (1)$$

in which m_i is the impulsive part of the liquid mass, m_s and m_b are respectively wall and base tank masses, and k_{iso} is the elastic stiffness of the isolators.

Often, the support structure is made of short RC columns and thus with a limited deformability. Consequently, Eq. (1) can be considered applicable in most of the cases. In addition, when elevated tanks are also very slender, the convective motion can be very restricted providing a limited contribution to the lateral pressure on the wall. The negative effect of the sloshing is related only to the superficial motion, because either the height of the wave can exceed the upper limit, causing overtopping phenomenon, or the floating roof motion could cause a breaking of the gaskets and the leakage of dangerous vapors of inflammable substances. Unfortunately, the base isolation does not modify this phenomenon.

2. DESCRIPTION OF THE CASE STUDY

As a case study, an emblematic example of elevated tanks collapsed during the Kocaeli Earthquake in 1999 at Habas Pharmaceutics plant in Turkey, has been considered [2].

The two damaged tanks on the left shown in Fig.3 contained liquefied oxygen while the undamaged tank on the right had liquefied nitrogen. Habas plant representatives on site reported that the liquefied oxygen tanks were 85% full and the liquefied nitrogen tank was about 25% full immediately before the earthquake. Each tank consisted of two concentric stainless steel shells, one with an outside diameter of 14.6 m and the other with an outside diameter of 12.8 m (shown in Fig.4). The gap between the inner and

outer shells was filled with perlite which is a form of natural glass (foam) and a lightweight insulating material.

The clear height of the tanks between the bottom slab and top stainless cover is about 12 m (shown in Fig.5). Thus, the volume of the tanks is approximately 1500 m^3. All tanks were supported on a 14.6 m-diameter, 1.07 m-thick RC slab that was in turn supported by sixteen 500 mm-diameter RC columns.

Figure 3. Storage tanks of Liquid Oxygen at Habas plant after the strong event of Izmit (1999)

Each column was 2.5 m in height and reinforced with sixteen 16 mm-diameter longitudinal bars and 8 mm-diameter ties spaced at approximately 100 mm on center. According to [2], the concrete used for the columns and the bottom slab was of class C30/37, whereas the steel bars had a yielding strength of 430 MPa. The density of the oxygen was 11.50 kN/m^3.

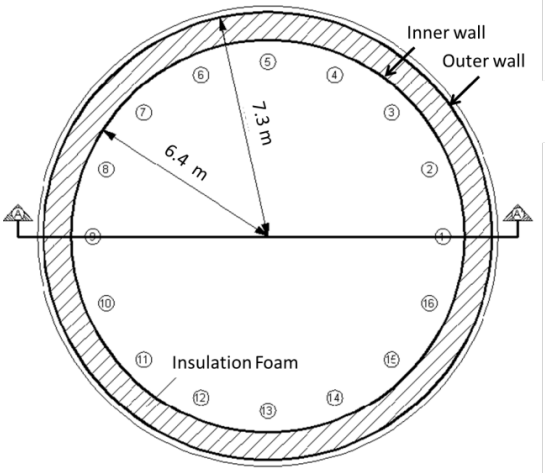

Figure 4. Plan view of the tank

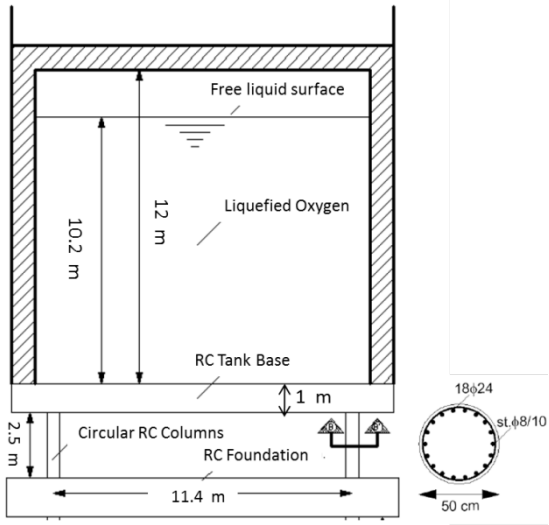

Figure 5. Section in the vertical plan of the tank

3. SEISMIC RESPONSE OF THE NON-ISOLATED TANK

3.1 Free vibration response

In order to determine the dynamic characteristics of the tank, the modal analysis of the non-isolated case has been performed. This allows to identify the relative importance of the components of the liquid motion (impulsive, convective, fluid-structure). The analysis resulted in the identification of the masses and stiffness shown in Fig.2 have been identified (Table 1).

Table 1. Dynamic properties of liquid and support

	Liquid		Support
	Impulsive	**Convective**	**Base**
Mass (t)	1062	428	510
Damping ratio (ξ)	2.0	0.5	5.0
Stiffness (kN/m)	174442	1233	196421

The convective and impulsive masses have been calculated according to the prescriptions of EC8 part 4 [12]:

$$\omega_c = \sqrt{1.841 \frac{g}{R} tanh(1.841 \frac{H}{R})} \tag{2}$$

$$\omega_i \approx \frac{C}{H} \sqrt{\frac{E\, s}{\rho\, R}} \tag{3}$$

While the expression of ω_c derives analytically from study of the liquid motion, the expression of ω_i is approximated [8]; ρ is the fluid density, s is the thickness of the tank wall and E is the young modulus of the material of which the tank wall is made of; the coefficient C depends on the ratio H/R and varies between 0.17 and 0.13 in common practice.

According to literature results [7], the damping ratio of impulsive and convective components of the motion have been chosen, respectively, equal to 2% and 0.5%.

In Table 2, the results of the modal analysis are reported in terms of vibration periods and participating masses (MPM) of the first three periods.

These results highlight the practical independency of the convective motion of the fluid (Mode 1) with respect to the impulsive motion. Period and MPM of the second mode, where the motion of impulsive mass is mainly involved, are instead slightly greater than the quantities indicated in Table 2; this is due to the presence of the base supports. In any case, the increasing of the period is a positive effect, which reduces the absolute accelerations and the inertia forces.

Table 2. Dynamic characteristics of the non-isolated tank

Mode	**1**	**2**	**3**
T(sec)	3.57	0.56	0.16
MPM (%)	22	64	14

3.2 Dynamic response analysis of the tank

For the evaluation of the seismic response of the tanks, time-history (T-H) analyses were conducted using the simplified model of Fig. 2, subjected to a series of natural records selected among a series of accelerograms recorded during the 1999 Kocaeli earthquake and listed in Table 3. They have been selected according to the following criteria:

- Soil type C, Soil factor S=1.15
- S-waves velocity between 180 m/s and 360 m/s
- distance d from the fault: 10< d < 30 km
- 0.20g < PGA < 0.35g

The response spectra of all unscaled records are shown in Fig. 6 together with the Elastic spectrum at Ultimate Limit State [13]. This latter has been established based on the class of the structure (Class IV) and consequently using an importance factor γ_I=*1.6*. As design ground acceleration a PGA=0.4 g on soil A has been selected.

Table 3. Set of natural records used for the T-H analysis

Accelerogram	Vs30 (m/s)	Distance (km)	PGA(g)
Yarimca330	297	5	0.349
Yarimca060	297	5	0.268
Faith090	228	55	0.159
Duzce270	276	15	0.358
Duzce180	276	15	0.312
Cekmece090	346	67	0.133
Cekmece000	346	67	0.179

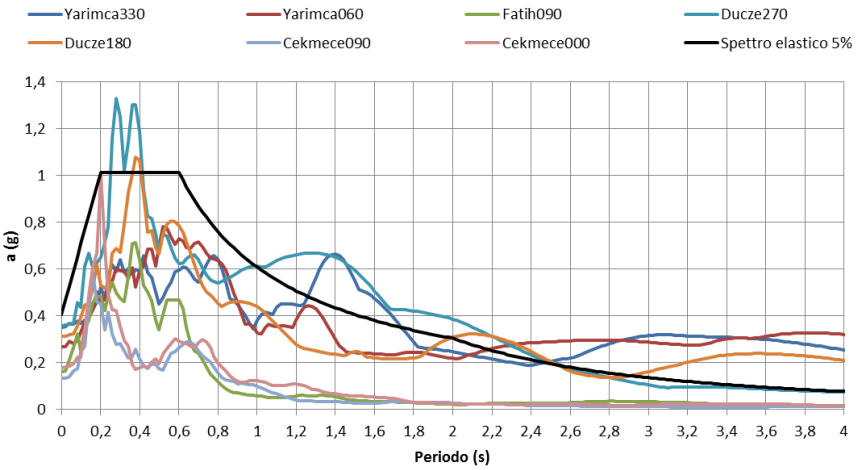

Figure 6. Response Spectra of the 7 unscaled accelerograms

In order to satisfy the compatibility conditions of accelerograms with the design spectrum [12], each record has been first scaled to minimize the mean square error and to obtain, around the fundamental period, a spectral ordinate equal to the design one.

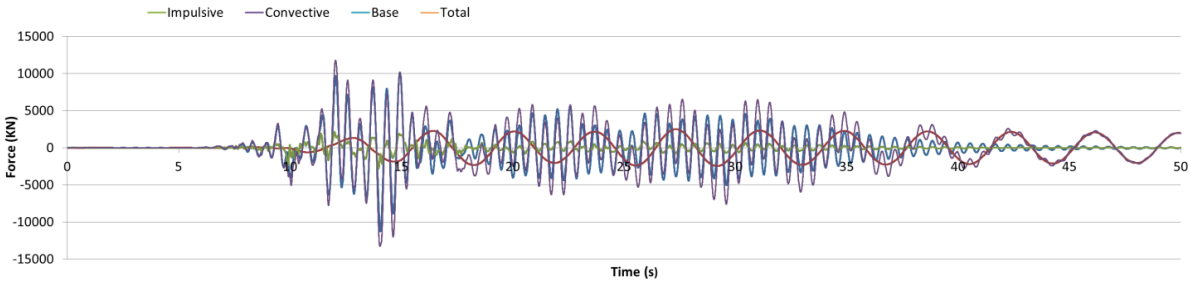

Figure 7. Non-Isolated case: Time-History of Base shear components for Yarimca 330 record

For each accelerogram a time-history analysis has been performed using SAP2000 software [14]. For each mass shown in Fig. 2 the absolute acceleration has been obtained together with the corresponding inertia forces. For example, the response in terms of base shear forces to one of the scaled accelerograms (Yarimca 330) is shown in Fig.7: in particular, the total base shear and the impulsive and convective components. In addition the force due to the mass placed at the tank base ($m_b+m_w+m_s$) is also shown. It can be noticed that:

- The motion of the convective mass is practically independent of the remaining masses as already confirmed by the modal analysis.
- In the steady-state condition, the total base shear coincides with the convective one, whose oscillations appear less damped.
- The impulsive mass undergoes higher accelerations than the tank base mass, indicating that the fluid-structure effect cannot be neglected.

The impulsive base shear is predominant with respect to the convective one (see Table 4).

Table 4. Maximum Base shear components – Non-isolated tank

Accelerogram	Impulsive (kN)	Convective (kN)	Base (kN)	Total (kN)
Yarimca330	10892	982	1390	13264
Yarimca060	13542	1753	2502	17796
Faith090	18062	100	2018	20079
Duzce270	10309	117	1596	11789
Duzce180	18573	541	2601	21715
Cekmece090	16534	291	3620	19863
Cekmece000	13011	91	3383	16303

Using the average value of maximum accelerations for each fluid motion component the corresponding distribution of the pressure on the wall has been evaluated and depicted in Fig. 8 for an angle θ=0°.

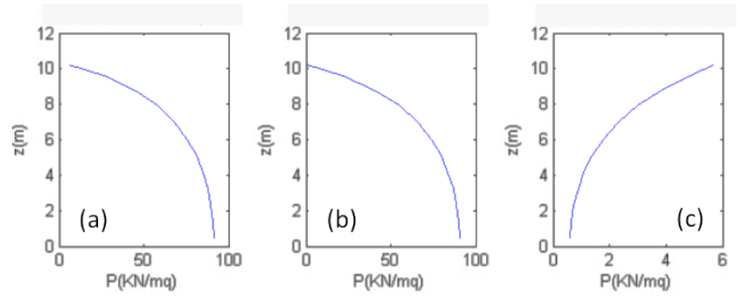

Figure 8. Non isolated case - average wall pressures (a) Total, (b) Impulsive, (c) Convective

Using maximum base shear, it has been possible to check support columns and wall against failure. In particular, according to the Turkish code [15], the maximum shear strength of the columns is about 330 kN [2], against a maximum shear action of about 1100 kN. This demonstrates the high vulnerability of these tanks as dramatically shown during the 1999 Kocaeli earthquake.

4. ISOLATED TANK: A COMPARISON BETWEEN FPS AND HDRB ISOLATORS

The results of the previous section suggested the use of a proper mitigation technique as the base isolation systems. Given that the few applications found in literature used either High Damping Rubber Bearings (HDRB) or Friction Pendulum (FP), in what follow their effectiveness in reducing the seismic response of the case study is studied and compared.

4.1 Seismic response of the tank isolated with HDRB

The HDRB isolators were designed for an isolation period T_{iso}=2.5 sec and a damping ratio ξ=10%. Consequently, using Eq.(1) the stiffness of the single device is k_{1iso} = 625 kN/m. Assuming a transversal modulus G=0.6 MPa, each isolator had a diameter D=450 mm and a total thickness of elastomeric layers t_e=153 mm, this latter was determined assuming a design shear deformation γ=100% and a design lateral displacement equal to 250 mm. The modal analysis of the isolated tank has been performed using the model shown in Fig. 2, where k_{iso}≅10000 kN/m and m_{iso}=9.8 ton. The results are shown in Table 5.

Table 5. Dynamic parameters of the isolated tank (HDRB)

Mode	1	2	3
T(sec)	4.10	2.34	0.28
MPM (%)	50%	49%	1

From these results, it can be drawn that:

- The fundamental period of the tank, where the impulsive motion was mainly involved, goes from 0.56 sec to 2.34 sec, with a consequent reduction of absolute accelerations. The obtained period is not exactly equal to T_{iso} given that the behavior of the tank is not perfectly rigid.
- The participating mass to the convective motion increases for the high deformability of the isolators for which it could result in a possible interaction between convective and isolated motion.
- The convective period remains practically unchanged, demonstrating how the isolation system does not affect the sloshing motion.

The seismic analysis of the isolated tank has been performed using the same accelerograms of Table 4. Anyhow, the scaling procedure has been performed considering as reference period T_{iso}. Using these accelerograms, a new time-history analysis has been performed. Fig. 9 shows again the response in terms of base shear components. Analyzing the T-H response, it can be noticed that:

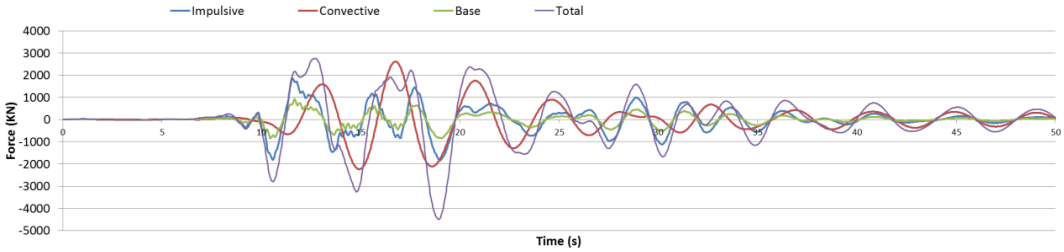

Figure 9. Isolated case - HDRB: Time-History of Base shear components for Yarimca record

- The base and impulsive mass accelerations are very similar, showing that the structure behaves rigidly during the motion
- The convective motion is again independent from the rest of the motion.
- The convective shear force assumes values similar to those of non-isolated case, whereas the impulsive force decreases up to 80%.

This is clearly shown in Table 6 where the maximum force of each mass is reported for each record. The mean total base shear is about 2900 kN against 18000 kN of the non-isolated case, and thus with a reduction of about 80%.

Table 6. Isolated case - HDRB: Maximum Base shear components

Accelerogram	Impulsive (kN)	Convective (kN)	Base (kN)	Total (kN)
Yarimca330	1795	1868	15	4498
Yarimca060	3040	2447	24	6767
Faith090	370	249	3	779
Duzce270	1840	458	20	2454
Duzce180	1402	1823	12	3880
Cekmece090	695	118	7	1203
Cekmece000	605	124	5	1013

The average pressure components acting on the wall are shown in Fig. 10. The maximum impulsive pressure is now reduced to 9 kN/m^2 from about 90 kN/m^2. This means that in all columns the shear force demand is highly reduced, obtaining now values well under the shear strength. Similarly, the convective pressure increases, remaining, in any case, confined within a range of low values. Finally, all necessary checks according to EC8 have been performed. Given that the average value of the maximum displacement of HDRB isolators is 0.28 m, the maximum deformation of the devices is attained. Using a different elastic

modulus (e.g. G=1.4 MPa), the deformability can be reduced, but in any case it remains extremely high. Consequently, in the next section, a different type of isolator has been proposed and investigated.

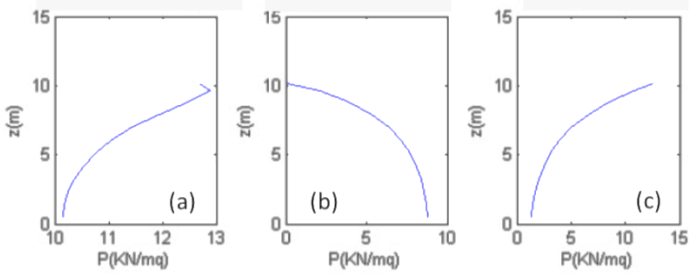

Figure 10. Isolated case HDRB - average wall pressures (a) Total, (b) Impulsive, (c) Convective

4.2 Seismic response of tank isolated with FPS and comparison with HDRB isolators

In this section, the seismic response of the tanks isolated with FPS bearings is investigated. For structures where the isolated mass comes from the entire weight, this typology represents an interesting solution because of the independency of the response from the mass itself. In fact, in this case the period can be calculated according to Eq. (4).

$$T_p = 2\pi \sqrt{\frac{m}{k_e}} = 2\pi \sqrt{\frac{m}{g\, m \left(\frac{1}{R} + \frac{\mu}{X}\right)}} = 2\pi \sqrt{\frac{1}{g \left(\frac{1}{R} + \frac{\mu}{X}\right)}} \tag{4}$$

In case where the participating mass to seismic motion is a fraction of the total mass, this independency is no longer verified. As a matter of fact, in case of storage tanks, the period is indicated in Eq.(5), where the dependency of the mass is clearly shown. The greater the convective mass, the lower the vibration period T_p. For example, in broad tanks; the sensibility of the response from the mass is higher than in slender tanks, for which the convective mass is usually a small part of the total mass of the fluid.

$$T_p = 2\pi \sqrt{\frac{m}{k_e}} = 2\pi \sqrt{\frac{m_{imp} + m_{ss} + m_{iso}}{g\, m_{tot} \left(\frac{1}{R} + \frac{\mu}{X}\right)}} \tag{5}$$

In the analyzed case study, the convective/impulsive mass ratio is about 50%, therefore the sensitivity of the response from the mass cannot be considered totally negligible. Considering a curvature Radius R=3175 mm, a friction coefficient of 3% and a maximum design displacement δ=350 mm and equivalent period $T_{eq}=3sec$ and a damping ratio $\xi=13.5\%$ are obtained.

To perform time-history analysis, the simplified non-linear model for FPS isolators implemented in SAP2000 has been used, which does not take into account the dependency of the response of the isolator from the vertical load.

For example, the response of the isolated tank to the Yarimca330 record, are shown in Fig. 11. From the results, it can be drawn that:

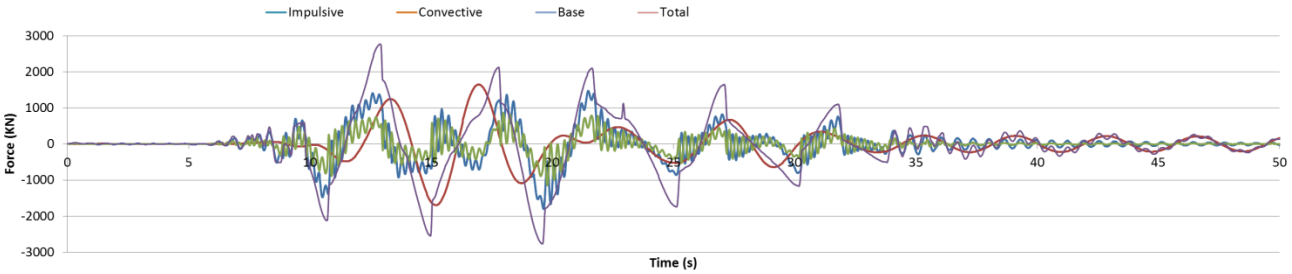

Figure 11. Isolated case - FPS: Time-History of Base shear components for Yarimca record

- The base and impulsive mass accelerations are very similar, showing that, as in the case of HDRB isolators, the structure behaves rigidly during the motion.
- The impulsive mass acceleration is substantially reduced with respect to the non-isolated case, showing the high effectiveness of the FPS isolation system
- The amplitude of the convective base shear seems to be reduced with respect to the HDRB isolators. This is probably due to a higher damping ratio (13.5%).
- The maximum total base shear is now reduced of 88%. This is justifiable by the increase of both equivalent period and damping ratio.

In Table 7, the maximum base shear is reported together with the maximum values of convective and impulsive shear forces. In this case, an average value of base shear of 2055 kN is obtained. This value is a little bit lower than 2900 obtained with HRDB isolator.

Table 7. Isolated case - FRP: Maximum Base shear components

Accelerogram	Impulsive (kN)	Convective (kN)	Base (kN)	Total (kN)
Yarimca330	1256	982	524	2772
Yarimca060	2201	1997	831	5045
Faith090	693	22	73	790
Duzce270	1182	69	117	1370
Duzce180	1232	681	492	2414
Cekmece090	857	207	90	973
Cekmece000	813	66	140	1021

The dissipation capability of the FPS bearings activated during the motion and the cyclic response for Yarimca330 record is shown in Fig. 12. The level of pressure acting on the wall during the earthquake is extremely reduced for HDRB isolators as shown in Fig. 13, where the average value of impulsive and convective component along the height are shown. The average value of the maximum displacements of FPS isolators is about 290 mm that is compatible with most of the commercial FPS bearings. This value is similar to the displacement obtained in case of HDRB isolator, with the difference that now it is fully compatible with the FPS isolation systems.

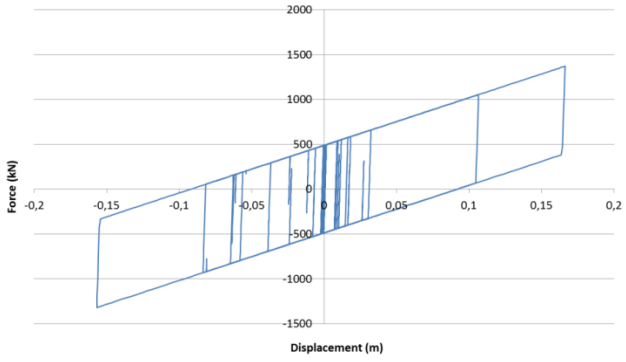

Figure 12. Cyclic response of an FPS isolator – Duzce270 record

The stress level in the wall in both the case is extremely limited. In particular, according to the EC8 Part 4 [12], the stresses corresponding to the elephant foot buckling and elastic buckling condition are 75 MPa and 104 MPa, respectively, whereas the maximum stress obtained from the T-H analysis is about 20.8 MPa and 17.4 MPa for HDRB and FPS isolators, respectively. Finally, the maximum vertical displacement due to the sloshing phenomenon is equal to 1.79 m and 1.13 m for HDRB and FPS isolators, respectively. This is fully compatible with the limit of 1.80 m imposed by the geometry. The lower value obtained using FPS isolators shows their better performance.

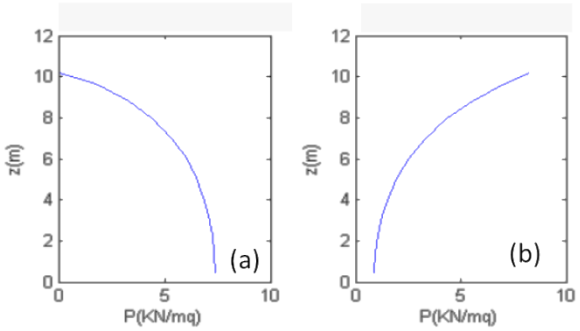

Figure 13. Isolated case FPS - Average wall pressures (a) Impulsive, (b) Convective

5. CONCLUSION

In this paper, the effectiveness of two type of isolation devices in reducing the seismic response of elevated tanks has been investigated. In particular, HDRB and FPS bearings have been analyzed. As a case study, an emblematic example of elevated tanks collapsed during the Kocaeli Earthquake in 1999 at Habas Pharmaceutics plant in Turkey, has been considered. The plant consisted of a group of three elevated tanks, containing liquefied oxygen and liquefied nitrogen. The two tanks with stored liquefied oxygen collapsed due to shear failure of the RC short columns that sustained the tank. The time-history analysis conducted using a lumped mass model demonstrated the high demand in terms of base shear required for the support columns and their inevitable collapse due to the insufficient shear strength. Consequently, the design of the above mentioned isolation systems was conducted and the response of the systems was investigated through time history analysis using lumped mass models properly modified to account for the presence of the isolation system. In particular, an equivalent model was adopted for HDRB, whereas the FPS bearing was modeled with a simplified non-linear model in which the influence of the vertical load on the later stiffness was neglected. The capability of both isolation systems in reducing the base shear and stress level in the wall has been clearly demonstrated. In particular, the reduction of about 80% and 88% of the total and impulsive base shears has shown the high effectiveness of both isolators. The use of HDRB was limited by the maximum displacement required by the seismic action, completely compatible with the FPS isolators. The reduction of the stress level eliminates any possible buckling phenomenon in the wall. Finally, the lower value of vertical sloshing displacements of the liquid obtained using FPS isolator suggests the adoption of sliding bearings rather than HDRB in seismic isolation of the elevated tanks.

ACKNOWLEDGMENTS

This work has been partially funded by the Italian RELUIS consortium within the executive research program 2010-2013 – research thrust 2 – Special Structures.

REFERENCES

[1] Paolacci F., Giannini R., De Angelis M., (2013), Seismic response mitigation of chemical plant components by passive control systems, Journal of Loss Prevention in Process Industries, Volume 26, Issue 5, Pages 879-948 DOI:10.1016/j.jlp.2013.03.003

[2] Sezen H, Lıvaoğlu R, Doğangün A. (2008), Dynamic analysis and seismic performance evaluation of above-ground liquid-containing tanks. Engineering Structures 30: 794– 803

[3] Housner G.W. (1963). The dynamic behaviour of water tanks. Bulletin of the Seismological Society of America, 53, 381-387

[4] Fischer D. (1979). Dynamic fluid effects in liquid-filled flexible cylindrical tanks. Earthquake Engineering and Structural Dynamics,7, 587-601

[5] Haroun M.A., Hausner G.W. (1981). Earthquake response of deformable liquid storage tanks. Journal of Applied Mechanics, 48, 411-418.

[6] Veletsos A.S., Tang Y. (1987). Rocking response of liquid storage tanks. Journal of Engineering Mechanics, 113, 1774-1792

[7] De Angelis M., Giannini R., Paolacci F., (2010), Experimental investigation on the seismic response of a steel liquid storage tank equipped with floating roof by shaking table tests, Earthquake Engineering & Structural Dynamics, 39: 377–396. DOI: 10.1002/eqe.945

[8] Wang Y., Teng M. and Chung K. (2001). Seismic isolation of rigid cylindrical tanks using friction pendulum bearings. Earthquake Engineering and Structural Dynamics, 30, 1083–1099

[9] Shrimali M.K., Jangid R.S. (2002). Non-linear seismic response of base-isolated liquid storage tanks to bi-directional excitation. Nuclear Engineering and Design. 217, 1–20.

[10] Tajirian F. F. (1998). Base isolation design for civil components and civil structures. Proceedings of Structural Engineers World Congress, San Francisco, California, July

[11] Calugaru, V., & Mahin, S. A. (2009). Experimental and analytical studies of fixed base and seismically isolated liquid storage tanks. In 3rd Int. conf. on advances in experimental structural engineering, October 15e16, 2009, San Francisco.

[12] EN 1998-4 (2006): Eurocode 8: Design of structures for earthquake resistance – Part 1: General rules, seismic actions and rules for buildings.

[13] EN 1998-1 (2004): Eurocode 8: Design of structures for earthquake resistance – Part 1: General rules, seismic actions and rules for buildings

[14] CSI Computer & Structures – SAP2000 – version 16.1

[15] Specification for Structures to be Built in Disaster Areas, Ministry of Public Works and Settlement Government of Republic of Turkey,2007